Draft version April 1, 2020
Typeset using LaTeX default style in AASTeX63

Calibrating gyrochronology using Galactic kinematics

Ruth Angus,[1,2,3] Yuxi (Lucy) Lu,[3,1] Dan Foreman-Mackey,[2] Adrian M. Price-Whelan,[2] Jason Curtis,[1] and Emily Cunningham[2]

[1]*Department of Astrophysics, American Museum of Natural History, 200 Central Park West, Manhattan, NY, USA*
[2]*Center for Computational Astrophysics, Flatiron Institute, 162 5th Avenue, Manhattan, NY, USA*
[3]*Department of Astronomy, Columbia University, Manhattan, NY, USA*

ABSTRACT

Gyrochronology, the method of inferring the age of a star from its rotation period, could provide ages for billions of stars over the coming decade of time-domain astronomy. However, the gyrochronology relations remain poorly calibrated due to a lack of precise ages for old, cool main-sequence stars. Now however, with proper motion measurements from Gaia, Galactic kinematics can be used as an age proxy, and the magnetic and rotational evolution of stars can be examined in detail. We demonstrate that kinematic ages, inferred from the velocity dispersions of groups of stars, beautifully illustrate the time and mass-dependence of the gyrochronology relations. We use the kinematic ages of field stars, plus benchmark clusters and asteroseismic stars, to calibrate a new empirical Gaussian process gyrochronology relation, that fully captures the complex rotational evolution of cool dwarfs over a range of masses and ages. We use cross validation to demonstrate that this relation accurately predicts ages for GKM dwarfs.

Keywords: Stellar Rotation — Stellar Evolution — Stellar Activity — Stellar Magnetic Fields — Low Mass Stars — Solar Analogs — Milky Way Dynamics

1. INTRODUCTION

Low mass dwarfs are the most common stars in the Milky Way, and their ages could reveal the evolution of Galactic stellar populations and planetary systems. However, the ages of GKM stars are difficult to measure because their luminosities and temperatures evolve slowly on the main sequence. Fortunately, rotation-dating, or 'gyrochronology' provides a promising means to measure precise ages for these cool dwarfs. The rotation periods of GKM stars evolve relatively rapidly, and a fully calibrated gyrochronology model that captures the time and mass-dependence of stellar spin down could provide ages that are precise to within 20% for millions of Milky Way stars in the time-domain era (Epstein & Pinsonneault 2014; Najita et al. 2016; Angus et al. 2019). However, gyrochronology models are not yet reliably calibrated, especially for low-mass and old stars.

With the thousands of new photometric rotation period measurements provided by specialized ground and space-based missions (particularly *Kepler*/*K2* and *TESS* Borucki et al. 2010; Howell et al. 2014; Ricker et al. 2015), we are making progress towards the ultimate goal for rotation-dating: a fully calibrated gyrochronology relation, applicable to GKM main-sequence stars of all ages. A lack of low-mass and old calibration stars has previously limited the mass and age coverage of gyrochronology relations, which can only be calibrated using stars with precise age and rotation period measurements. Historically, the gyrochronology calibration sample has been limited to open clusters and asteroseismic stars. Open clusters can be precisely dated with isochrone fitting and main sequence turn off, Solar-like oscillators can be dated by measuring their internal sound speed through frequency analysis, and the rotation periods of both cluster and asteroseismic stars can be measured with precise time-series photometry. Magnetically active regions create inhomogeneous surface features with rotate in and out of view and produce periodic variability in their integrated, broad-band emission. Measuring rotation periods from light curves is a research topic in and of itself, but many studies have successfully measured the rotation periods of thousands of stars in clusters and in the field, from *Kepler*, *K2*, and *TESS* light curves.

For the purposes of calibrating gyrochronology, open clusters provide good mass coverage for young stars: rotation periods have been measured for F through mid M dwarfs for stars in clusters with precisely measured ages up to around 700 Myr. Asteroseismic stars provide reasonable age coverage for hot stars: seismic masses and photometric surface rotation periods have been measured for F, G and early K dwarfs for stars as old as 10 Gyr. However, neither asteroseismology nor cluster analysis can provide rotation periods and ages for old, late K and M dwarfs. In addition, cluster and asteroseismic stars generally provide sparse coverage of the rotation period-effective temperature plane, and cannot reveal the detailed evolution of stellar rotation rates. As a result, most empirical gyrochronology relations are only reliable for G dwarfs up to Solar age, K dwarfs up to 2-3 Gyr, and early M dwarfs up to < 1 Gyr. For this reason, the rotational evolution of cool dwarfs is not well understood. However, as we showed in Angus *et al.* (2020), the *kinematic* ages of field stars observed by *Kepler*, can provide a calibration sample with broad mass and age coverage. Although the *Kepler* sample does not include late M dwarfs, it can still be used to extend gyrochronology relations to much older ages for late K and early M dwarfs. By adding the ages and rotation periods of thousands of field stars to the open cluster and asteroseismic calibration sample, we can calibrate a gyrochronology relation that is applicable to FGK and early M dwarfs between the ages of $\sim$500 Myr and 8 Gyr.

1.1. *Core-envelope decoupling*

In Angus *et al.* (2020) we demonstrated that Galactic kinematics can be used to explore the evolution of stellar rotation. We showed that velocity dispersion, an established age proxy in the Galactic thin disk, increases smoothly as a function of rotation period, indicating that rotation period increases with age as expected. Using velocity dispersion as an age proxy, we also showed that old K dwarfs spin down more slowly than G dwarfs: their rotational evolution appears to 'stall' after around 1 Gyr, in a manner that reflects the behavior of K dwarfs observed in open clusters (Curtis et al. 2019). At young ages ($\sim 0.5-1$ Gyr), K dwarfs spin more slowly than G dwarfs of the same age, because their deeper convection zones generate stronger magnetic fields, which leads to more efficient magnetic braking. However, at old ages ($\gtrsim 1$ Gyr) K dwarfs rotate at the same rate or more rapidly than contemporary G dwarfs. The leading explanation for this phenomenon is that angular momentum is transferred from the core to the surface over longer timescales for lower-mass stars (Spada & Lanzafame 2019), *i.e.* they experience a more extended phase of 'core-envelope decoupling'.

A period of core-envelope decoupling is necessary to explain the observed rotation periods of stars in extremely young open clusters (1-10 Gyr) (*e.g.* Irwin et al. 2007; Bouvier 2008; Denissenkov et al. 2010; Spada et al. 2011; Reiners & Mohanty 2012; Gallet & Bouvier 2013). During this phase there is little transfer of angular momentum between radiative core and convective envelope and, as wind-braking removes angular momentum from the envelope, it decelerates while the core continues to spin rapidly. Over time however, angular momentum is transported across the interface between the two zones, and momentum from the rapidly spinning interior surfaces, inhibiting the deceleration of the outer envelope. Currently, the rotation periods of field and cluster stars can only be reproduced by semi-empirical models with a mass-dependent timescale for core-envelope coupling (Spada & Lanzafame 2019; Curtis et al. 2019, Angus *et al.*, 2020).

1.2. *Using kinematics as an age proxy*

The star forming molecular gas clouds observed in the Milky Way have a low out-of-plane, or vertical, velocity (*e.g.* Stark & Brand 1989; Stark & Lee 2005; Aumer & Binney 2009; Martig et al. 2014; Aumer et al. 2016). In contrast, the vertical velocities of older stars are observed to be larger in magnitude on average (Strömberg 1946; Wielen 1977; Nordström et al. 2004; Holmberg et al. 2007, 2009; Aumer & Binney 2009; Casagrande et al. 2011; Ting & Rix 2019; Yu & Liu 2018). There are two possible explanations for this observed increase in velocity dispersion with age: either stars are born kinematically 'cool' and their orbits are heated over time via interactions with giant molecular clouds (see Sellwood 2014, for a review of secular evolution in the MW), or stars formed kinematically 'hotter' in the past (*e.g.* Bird et al. 2013). Either way, the vertical velocity dispersions of thin disk stars are observed to increase with stellar age. This behavior is codified by Age-Velocity dispersion Relations (AVRs), which typically express the relationship between age and velocity dispersion as a power law: $\sigma_v \propto t^\beta$, with free parameter, β (*e.g.* Holmberg et al. 2009; Yu & Liu 2018). These expressions can be used to infer the ages of groups of stars from their velocity dispersions, as we do in this paper (see section 2).

Kinematic ages have been used to explore the evolution of cool dwarfs for over a decade. West et al. (2004, 2006) found that the fraction of magnetically active M dwarfs decreases over time, by using the vertical distances of stars from the Galactic mid-plane as an age proxy, and West et al. (2008) used kinematic ages to calculate the expected activity lifetime for M dwarfs of different spectral types. Faherty et al. (2009) used tangential velocities to infer the ages of M, L and T dwarfs, and showed that dwarfs with lower surface gravities tended to be kinematically younger, and Kiman et al. (2019) used velocity dispersion as an age proxy to explore the evolution of Hα equivalent width (a magnetic activity indicator), in M dwarfs.

AVRs are usually calibrated in Galactocentric velocity coordinates ($v_{\mathbf{x}}$, $v_{\mathbf{y}}$, $v_{\mathbf{z}}$ or UVW), and these velocities can only be calculated with full 6D positional and velocity information, however most *Kepler* rotators do not have RV measurements[1]. In Angus *et al.* (2020) we used velocity in the direction of Galactic latitude ($v_{\mathbf{b}}$) as a stand-in for $v_{\mathbf{z}}$ because, in the *Galactic* coordinate system, velocities can be calculated from 3D positions and *2D* proper motions. The *Kepler* field lies at low Galactic latitude, so $v_{\mathbf{b}}$ is a close approximation to $v_{\mathbf{z}}$. Though $v_{\mathbf{b}}$ velocity dispersion does not equal $v_{\mathbf{z}}$ velocity dispersion, it still increases monotonically over time and provides accurate age rankings for *Kepler* stars. Unfortunately however, given that AVRs are calibrated in *Galactocentric* coordinates ($v_{\mathbf{x}}$, $v_{\mathbf{y}}$, $v_{\mathbf{z}}$), we could not directly translate $v_{\mathbf{b}}$ velocity dispersions to ages.

In this paper, our aim was to use kinematic ages to calibrate a new gyrochronology relation, for which four main steps were required. Firstly, we inferred *vertical* velocity, $v_{\mathbf{z}}$, for each star without an RV measurement by marginalizing over missing RVs using a hierarchical Bayesian model (see section 2.3). Secondly, we calculated velocity dispersion for every star using a moving, or rolling dispersion method (see section 2.2). Thirdly, these velocity dispersions were converted into ages using an AVR (Yu & Liu 2018, section **??**). Finally, we used a Gaussian process model to capture the complexities of stellar rotational evolution and calibrated a new gyrochronology relation using our kinematic ages, plus benchmark cluster and asteroseismic stars in section **??**.

[1] Although RVs for most will be released in *Gaia* DR3

2. METHOD

2.1. *Data*

This study focuses on stellar rotation in the original *Kepler* field. This is partly because *Kepler* provides the largest sample of published, homogeneously measured rotation periods, and partly because its low Galactic latitude allows us to marginalize over missing RV measurements and approximate vertical velocity, $v_{\mathbf{z}}$.

We combined two large rotation period catalogs constructed from original *Kepler* data: McQuillan et al. (2014) and Santos et al. (2019). The McQuillan et al. (2014) and Santos et al. (2019) studies used different techniques to measure rotation periods from *Kepler* light curves: autocorrelation functions and wavelets respectively. The Santos et al. (2019) study was specifically focused on cooler stars: K and M dwarfs, and includes a larger number of rotation periods for these stars. The combined catalogs provide a total of 36,000 rotation periods: ∼34,000 from McQuillan et al. (2014) and 2000 from Santos et al. (2019).

To calculate kinematic ages for stars with measured rotation periods, an estimate of vertical velocity, $v_{\mathbf{z}}$, is required. The ideal way to calculated $v_{\mathbf{z}}$ and similarly, $v_{\mathbf{x}}$ and $v_{\mathbf{y}}$, is to use 6D positional and velocity information. Many stars in the *Kepler* field do not have RV measurements and an alternative approach must be taken to infer their vertical velocities (see section 2.3). However, a large number of *Kepler* rotators, over 10,000 of 34,000 *do* have RV measurements from *Gaia* DR2 and *LAMOST*. Figure 1 shows rotation period vs effective temperature for all stars in the McQuillan et al. (2014) and Santos et al. (2019) catalogs, plotted in grey. Stars with RV measurements are colored by their vertical velocity dispersion (see section 2.2 to see how we calculated velocity dispersion). Although RVs are available for a significant number of *Kepler* rotators (almost one in three), few stars cooler than 4000 K have RV measurements. This is due to the faint limits of the *Gaia* DR2 and *LAMOST* surveys (although RV measurements for fainter targets will be available in *Gaia* DR3). Given that magneto-rotational evolution is poorly understood for M dwarfs, the cool stars with missing RVs are arguably the ones we care most about. For this reason, we attempt to compensate for the lack of RV measurements by inferring vertical velocities for stars without RVs, filling in the low-temperature region of figure 1 in section 2.3.

2.2. *Calculating velocity dispersions*

A kinematic age can be calculated from the velocity dispersion (*e.g.* the standard deviation or Median Absolute Deviation, MAD, of velocities) of a group of stars. These velocity dispersions can then be converted into an age using an AVR (*e.g.* Holmberg et al. 2009; Yu & Liu 2018). The major assumption underlying kinematic ages is that all stars used to calculate a velocity dispersion are *the same age*. So, in order to calculate kinematic ages from velocity dispersions for *Kepler* stars, it is necessary to group them by age. Fortunately, we can use the implicit assumption that underpins gyrochronology itself to group stars by age: that stars with the same rotation period and color are the same age. We discuss the implications of this assumption, and how our results would change if this assumption is false, in the Discussion of this paper (section **??**).

To calculate a $v_{\mathbf{z}}$ velocity dispersion and therefore age for each *Kepler* star, we grouped stars with their neighbors in $\log(P_{\rm rot})$–$T_{\rm eff}$ space. We experimented with two methods of grouping stars: using K-nearest neighbors, and using a fixed range in $\log(P_{\rm rot})$ and $T_{\rm eff}$. In the K-nearest neighbors method, each star was grouped with the K-nearest stars in $\log(P_{\rm rot})$-$T_{\rm eff}$ space. Groups created this way span a small range of $\log(P_{\rm rot})$ and $T_{\rm eff}$ where the number density of stars is large, and a large range where the number density is small. However, all groups have the same number of stars. In the fixed range method, each star was grouped with stars whose $\log(P_{\rm rot})$s and $T_{\rm eff}$s fell within a certain range of their own. This method created groups with large numbers of stars in densely populated regions of the $\log(P_{\rm rot})$–$T_{\rm eff}$ plane, and small numbers of stars in sparsely populated regions, *i.e.* each group contains a different number of stars. However, the bin size was constant. To choose the best method, and to optimize for the parameters of each (K and $\log(P_{\rm rot})$ and $T_{\rm eff}$-range), we conducted a set of tests.

2.3. *Inferring 3D velocities (marginalizing over missing RV measurements)*

It has been demonstrated that the dispersion in vertical velocity, $v_{\mathbf{z}}$ for a group of stars increases with the age of that group (citations). However, velocities in Galactocentric coordinates, $v_{\mathbf{x}}$, $v_{\mathbf{y}}$ and $v_{\mathbf{z}}$, can only be calculated with full 6-D position and velocity information, *i.e.* proper motions, position and radial velocity. In Angus *et al.* (2020) we introduced the idea that kinematic ages could be used to calibrate gyrochronology and showed, in the appendix of that paper, that velocity, $v_{\mathbf{b}}$ in the Galactic frame, which can be calculated without an RV measurement, can be used as an approximation to $v_{\mathbf{z}}$ for *Kepler* stars. This is because the *Kepler* field of view lies at relatively low Galactic latitudes,

Figure 1. Vertical velocity dispersion as a function of rotation period and effective temperature for *Kepler* stars with measured rotation periods. Colored points show stars with RV measurements from *Gaia* or *LAMOST*. Faint grey points show the combined McQuillan et al. (2014) and Santos et al. (2019) samples, including stars without RV measurements. The coolest stars in this sample do not have RVs because they are faint.

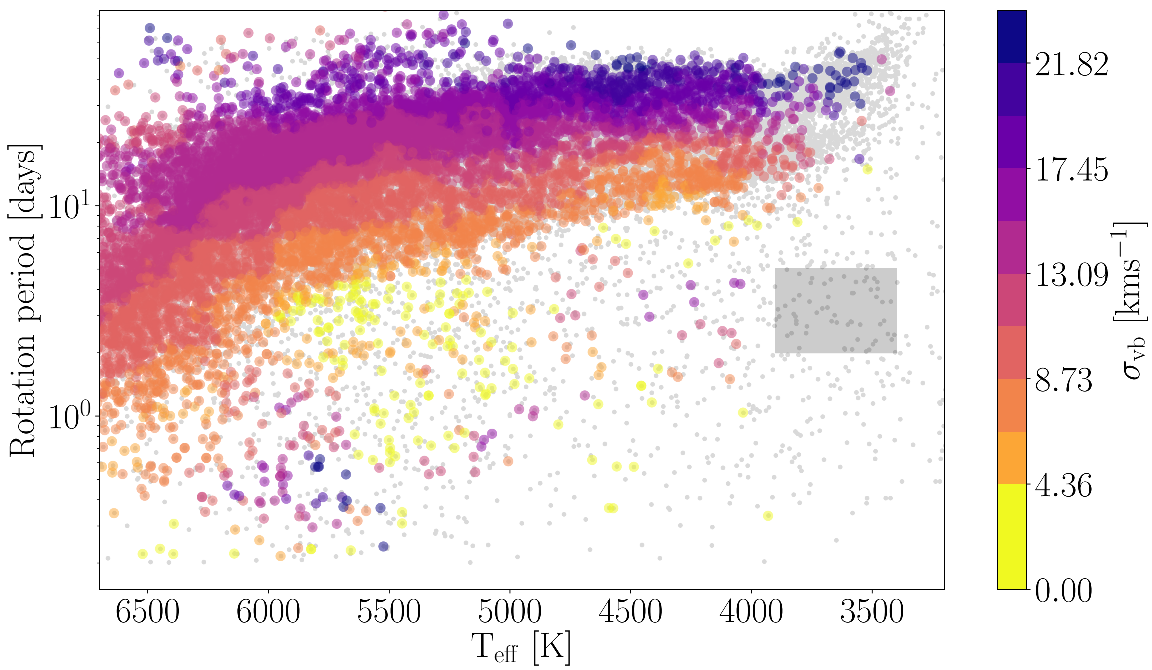

($\sim 5-20^{\circ}$), so the z-direction is similar to the b-direction for *Kepler* stars. However, $v_{\mathbf{b}}$ is only a close approximation to $v_{\mathbf{z}}$ at extremely *low* latitudes, and even in the *Kepler* field, kinematic ages calculated with $v_{\mathbf{b}}$ instead of $v_{\mathbf{z}}$ are systematically larger because of extra noise introduced by the imperfect translation between $v_{\mathbf{b}}$ and $v_{\mathbf{z}}$İn order to calculate accurate vertical velocities and therefore ages, the appropriate approach is to *infer* $v_{\mathbf{z}}$ by marginalizing over missing RV measurements.

Three-dimensional velocities in galactocentric coordinates: $v_{\mathbf{x}}$, $v_{\mathbf{y}}$, and $v_{\mathbf{z}}$ can only be directly computed via a transformation from 3D velocities in another coordinate system, like the equatorial coordinates provided by *Gaia*: μ_{α}, μ_{δ}, and RV. For stars with no measured RV in *Gaia* DR2, $v_{\mathbf{x}}$, vy, and $v_{\mathbf{z}}$ can still be inferred from positions and proper motions alone, by marginalizing over missing RV measurements. For each star in our sample, we inferred $v_{\mathbf{x}}$, $v_{\mathbf{y}}$, and $v_{\mathbf{z}}$ from the 3D positions and proper motions provided in the *Gaia* DR2 catalog (Brown et al. 2011). We also simultaneously inferred distance, instead of using $1/\pi$, to model velocities (Bailer-Jones 2015; Bailer-Jones et al. 2018).

Using Bayes rule, the posterior probability of the parameters given the data can be written:

$$p(v_{\mathbf{xyz}}, D|\mu_{\alpha}, \mu_{\delta}, \alpha, \delta, \pi) = p(\mu_{\alpha}, \mu_{\delta}, \alpha, \delta, \pi|v_{\mathbf{xyz}}, D)p(v_{\mathbf{xyz}})p(D), \tag{1}$$

where D is distance, α is Right Ascension (RA), δ is declination (dec), π is parallax, μ_{α} is proper motion in RA, and μ_{δ} is proper motion in dec. The prior over log(distance) and velocities was a multivariate Gaussian with mean and covariance determined from the distance and velocity distributions of *Kepler* targets with RV measurements.

The posterior PDF was explored using `emcee` (Foreman-Mackey et al. 2013), an affine-invariant, ensemble MCMC sampler.

Initialization.

We found that 10,000 samples with 16 walkers was sufficient to calculate a converged autocorrelation time, and produce 150-500 independent samples per parameter.

Over 3000 stars in the McQuillan et al. (2014) sample do have RV measurements and provide an opportunity to test this method of inferring velocities. Figure **??** shows the velocities of these 3000 stars, calculated using RV measurements, compared with their inferred velocities.

Figure 2. Vertical velocities calculated with full 6D information vs vertical velocities inferred without RV, for all 3000 McQuillan et al. (2014) stars with *Gaia* RV measurements.

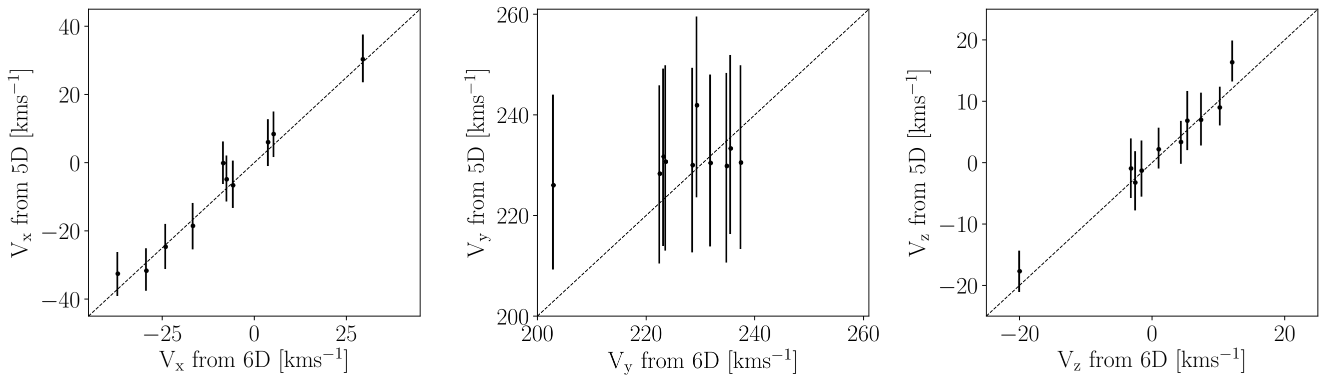

2.4. *Converting velocity dispersion to age with an AVR*

2.5. *Comparing kinematic ages with asteroseismic and cluster ages*

2.6. *A Gaussian process gyrochronology relation*

3. RESULTS

4. DISCUSSION

5. CONCLUSION

This work was partly developed at the 2019 KITP conference ‘Better stars, better planets’. Parts of this project are based on ideas explored at the Gaia sprints at the Flatiron Institute in New York City, 2016 and MPIA, Heidelberg, 2017. This work made use of the gaia-kepler.fun crossmatch database created by Megan Bedell.

Some of the data presented in this paper were obtained from the Mikulski Archive for Space Telescopes (MAST). STScI is operated by the Association of Universities for Research in Astronomy, Inc., under NASA contract NAS5-26555. Support for MAST for non-HST data is provided by the NASA Office of Space Science via grant NNX09AF08G and by other grants and contracts. This paper includes data collected by the Kepler mission. Funding for the *Kepler* mission is provided by the NASA Science Mission directorate.

This work has made use of data from the European Space Agency (ESA) mission *Gaia* (https://www.cosmos.esa.int/gaia), processed by the *Gaia* Data Processing and Analysis Consortium (DPAC, https://www.cosmos.esa.int/web/gaia/dpac/consortium). Funding for the DPAC has been provided by national institutions, in particular the institutions participating in the *Gaia* Multilateral Agreement.

REFERENCES

Angus, R., Morton, T. D., & Foreman-Mackey *et al*, D. 2019, AJ, 158, 173, doi: 10.3847/1538-3881/ab3c53

Aumer, M., Binney, J., & Schönrich, R. 2016, MNRAS, 462, 1697, doi: 10.1093/mnras/stw1639

Aumer, M., & Binney, J. J. 2009, MNRAS, 397, 1286, doi: 10.1111/j.1365-2966.2009.15053.x

Bailer-Jones, C. A. L. 2015, PASP, 127, 994, doi: 10.1086/683116

Bailer-Jones, C. A. L., Rybizki, J., & Fouesneau *et al*, M. 2018, AJ, 156, 58, doi: 10.3847/1538-3881/aacb21

Bird, J. C., Kazantzidis, S., & Weinberg *et al*, D. H. 2013, ApJ, 773, 43, doi: 10.1088/0004-637X/773/1/43

Borucki, W. J., Koch, D., & Basri *et al*, G. 2010, Science, 327, 977, doi: 10.1126/science.1185402

Bouvier, J. 2008, A&A, 489, L53, doi: 10.1051/0004-6361:200810574

Brown, T. M., Latham, D. W., & Everett *et al*, M. E. 2011, AJ, 142, 112, doi: 10.1088/0004-6256/142/4/112

Casagrande, L., Schönrich, R., & Asplund *et al*, M. 2011, A&A, 530, A138, doi: 10.1051/0004-6361/201016276

Curtis, J. L., Agüeros, M. A., & Douglas *et al*, S. 2019, arXiv e-prints. https://arxiv.org/abs/1905.06869

Denissenkov, P. A., Pinsonneault, M., & Terndrup *et al*, D. M. 2010, ApJ, 716, 1269, doi: 10.1088/0004-637X/716/2/1269

Epstein, C. R., & Pinsonneault, M. H. 2014, ApJ, 780, 159, doi: 10.1088/0004-637X/780/2/159

Faherty, J. K., Burgasser, A. J., & Cruz *et al*, K. L. 2009, AJ, 137, 1, doi: 10.1088/0004-6256/137/1/1

Foreman-Mackey, D., Hogg, D. W., & Lang *et al*, D. 2013, PASP, 125, 306, doi: 10.1086/670067

Gallet, F., & Bouvier, J. 2013, A&A, 556, A36, doi: 10.1051/0004-6361/201321302

Holmberg, J., Nordström, B., & Andersen, J. 2007, A&A, 475, 519, doi: 10.1051/0004-6361:20077221

—. 2009, A&A, 501, 941, doi: 10.1051/0004-6361/200811191

Howell, S. B., Sobeck, C., & Haas *et al*, M. 2014, PASP, 126, 398, doi: 10.1086/676406

Irwin, J., Hodgkin, S., & Aigrain *et al*, S. 2007, MNRAS, 377, 741, doi: 10.1111/j.1365-2966.2007.11640.x

Kiman, R., Schmidt, S. J., & Angus *et al*, R. 2019, AJ, 157, 231, doi: 10.3847/1538-3881/ab1753

Martig, M., Minchev, I., & Flynn, C. 2014, MNRAS, 443, 2452, doi: 10.1093/mnras/stu1322

McQuillan, A., Mazeh, T., & Aigrain, S. 2014, ApJS, 211, 24, doi: 10.1088/0067-0049/211/2/24

Najita, J., Willman, B., & Finkbeiner *et al*, D. P. 2016, arXiv e-prints, arXiv:1610.01661. https://arxiv.org/abs/1610.01661

Nordström, B., Mayor, M., & Andersen *et al*, J. 2004, A&A, 418, 989, doi: 10.1051/0004-6361:20035959

Reiners, A., & Mohanty, S. 2012, ApJ, 746, 43, doi: 10.1088/0004-637X/746/1/43

Ricker, G. R., Winn, J. N., & Vanderspek *et al*, R. 2015, Journal of Astronomical Telescopes, Instruments, and Systems, 1, 014003, doi: 10.1117/1.JATIS.1.1.014003

Santos, A. R. G., García, R. A., & Mathur *et al*, S. 2019, ApJS, 244, 21, doi: 10.3847/1538-4365/ab3b56

Sellwood, J. A. 2014, Reviews of Modern Physics, 86, 1, doi: 10.1103/RevModPhys.86.1

Spada, F., & Lanzafame, A. C. 2019, arXiv e-prints, arXiv:1908.00345. https://arxiv.org/abs/1908.00345

Spada, F., Lanzafame, A. C., & Lanza *et al*, A. F. 2011, MNRAS, 416, 447, doi: 10.1111/j.1365-2966.2011.19052.x

Stark, A. A., & Brand, J. 1989, ApJ, 339, 763, doi: 10.1086/167334

Stark, A. A., & Lee, Y. 2005, ApJL, 619, L159, doi: 10.1086/427936

Strömberg, G. 1946, ApJ, 104, 12, doi: 10.1086/144830

Ting, Y.-S., & Rix, H.-W. 2019, ApJ, 878, 21, doi: 10.3847/1538-4357/ab1ea5

West, A. A., Bochanski, J. J., & Hawley *et al*, S. L. 2006, AJ, 132, 2507, doi: 10.1086/508652

West, A. A., Hawley, S. L., & Bochanski *et al*, J. J. 2008, AJ, 135, 785, doi: 10.1088/0004-6256/135/3/785

West, A. A., Hawley, S. L., & Walkowicz *et al*, L. M. 2004, AJ, 128, 426, doi: 10.1086/421364

Wielen, R. 1977, A&A, 60, 263

Yu, J., & Liu, C. 2018, MNRAS, 475, 1093, doi: 10.1093/mnras/stx3204